Dependence of Climate Sensitivity on the Given Distribution of Relative Humidity

S. Bourdin[1,2], **L. Kluft**[1,3,4], **B. Stevens** [1]

[1]Max-Planck Institute for Meteorology, Hamburg, Germany
[2]Laboratoire des Sciences du Climat et de l'Environnement, LSCE/IPSL, CEA-CNRS-UVSQ, Université Paris-Saclay, Gif-sur-Yvette, F-91191, France
[3]International Max Planck Research School on Earth System Modelling
[4]Universität Hamburg, Faculty of Mathematics, Informatics and Natural Sciences, Department of Earth Sciences, Meteorological Institute, Hamburg, Germany

Key Points:

- Climate sensitivity is sensitive to the assumed distribution of relative humidity.
- Different relative humidity profiles explain clear-sky climate sensitivity spread among models.
- Tropical relative humidity trend in reanalyses yields an increase in climate sensitivity.

Corresponding author: Stella Bourdin, `stella.bourdin@lsce.ipsl.fr`

Abstract

We study how the vertical distribution of relative humidity (RH) affects climate sensitivity, even if it remains unchanged with warming. Using a radiative-convective equilibrium model, we show that the climate sensitivity depends on the shape of a fixed vertical distribution of humidity, tending to be higher for atmospheres with higher humidity. We interpret these effects in terms of the effective emission height of water vapor. Differences in the vertical distribution of RH are shown to explain a large part of the 10 % to 30 % differences in clear-sky sensitivity seen in climate and storm-resolving models. The results imply that convective aggregation reduces climate sensitivity, even when the degree of aggregation does not change with warming. Combining our findings with relative humidity trends in reanalysis data shows a tendency toward Earth becoming more sensitive to forcing over time. These trends and their height variation merit further study.

Plain Language Summary

Equilibrium Climate Sensitivity is the change in surface temperature in response to a doubling of atmospheric CO_2. We study how the assumed vertical distribution of relative humidity affects this sensitivity. Theoretical considerations show that the more moist an atmosphere is, the more it warms as a response to an increase in CO_2. Adding water vapor to the lower troposphere has the counter effect, lowering the sensitivity. We emphasize the importance of climate simulations taking humidity into account, as it is largely responsible for the difference in projections among models without clouds. We note surprising trends in humidity – with substantial drying of the lower troposphere over the ocean – in the last four decades as reported by two reanalyses of meteorological observations. Subject to the accuracy of these reconstructions, there appears to be a change with less moistening than expected, but with moistening/drying profiles which will condition Earth to become more sensitive to forcing over time. We stress the need for a study of observations to more critically evaluate these trends, and know better what models should aim for.

1 Introduction

The clear-sky response to an increase in greenhouse gases is a pillar of our understanding of global warming (Manabe & Wetherald, 1967; Charney et al., 1979). It is generally believed that this response is better described by an atmosphere whose relative, rather than absolute, humidity remains constant with warming. The distinction is crucial because in an atmosphere where RH is fixed, the response of surface temperature to radiative forcing (e.g., from changing CO_2), is roughly twice as large as would be the case should absolute humidity be fixed. In an influential review of these matters, Held and Soden (2000) presented theoretical arguments and evidence from modelling in support of a constant relative humidity. At the time of their review, observations were insufficient to test this hypothesis, but Held and Soden concluded that "10 years may be adequate, and 20 years will very likely be sufficient, [...] to convincingly confirm or refute the predictions". It is now twenty years later.

Taken at face value, two reanalyses of meteorological observations support this point of view, albeit less convincingly than we anticipated. This is shown in Fig. 1, where above 600 hPa RH is increasing with warming, at a rate of 1 %/decade to 4 %/decade.Rather than attempting to establish the reliability of the trends – a task for which we lack expertise – our aim is to estimate their implication for how Earth's equilibrium climate sensitivity may be changing. How does a moister upper, or drier lower, troposphere make Earth more or less sensitive to forcing? Posing this question raises even more basic questions. For instance, to what extent does the given structure of the RH profile matter for the clear-sky climate sensitivity, even if it remains constant with warming?

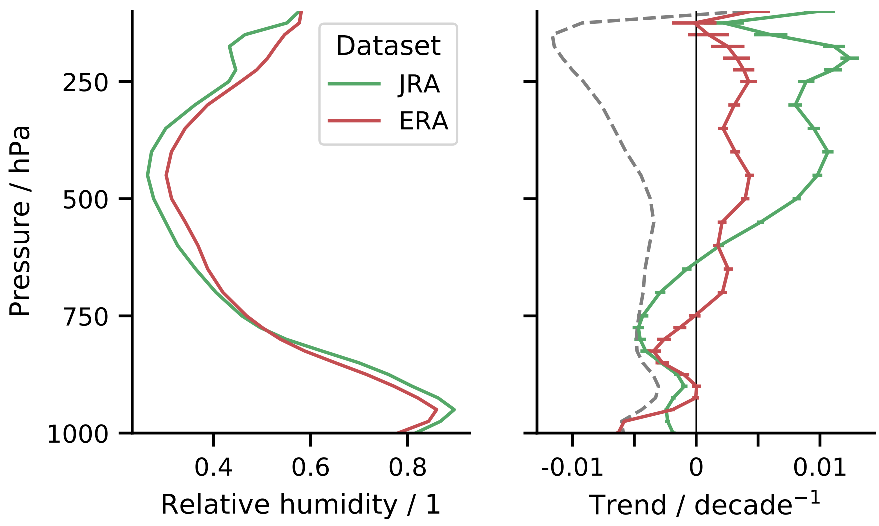

Figure 1. Mean profile (left) and linear trend over 40 years (solid, right) for ERA5 and JRA-55 reanalysis data. Error bars show the standard deviation of the linear regression. The grey dashed line corresponds to what would be the trend in relative humidity for a constant absolute humidity considering ERA5 tropical temperature trend.

Questions such as these have not been the topic of much study. Past work has focused on cloud changes (Stevens et al., 2016; Sherwood et al., 2020), to a degree that can give the impression that clouds alone stand in the way of a meaningful quantification of how surface temperatures respond to radiative forcing. This impression is reinforced by observations showing that outgoing long-wave radiation (OLR) varies linearly with temperature (Koll & Cronin, 2018), seeming to imply little role for RH. Looking beyond the inability of present climate models to represent clouds with fidelity, it is well known that: (i) water vapor strongly influences the radiation emitted from clear skies, and (ii) uncertainty in the clear-sky climate sensitivity is not negligible. Regarding (i), for the same thermal structure, OLR varies by more than $50\,\mathrm{W\,m^{-2}}$ with RH for present day tropical surface temperatures (Pierrehumbert, 1995). As for (ii), Soden and Held (2006) – the study often cited as being demonstrative of the constancy of clear-sky feedbacks – reports a range of $0.5\,\mathrm{W\,m^{-2}\,K^{-1}}$ in the combined water-vapor and lapse rate feedbacks across CMIP3 models. CMIP5 models show a smaller, but still appreciable ($0.4\,\mathrm{W\,m^{-2}\,K^{-1}}$), spread (Vial et al., 2013). More disquieting are studies that isolate the response of the tropical atmosphere to warming, as these suggest an even larger uncertainty (Medeiros et al., 2008; Becker & Wing, 2020). Relatively little research has been carried out to identify the origins of this uncertainty. Exceptional is the study by Po-Chedley et al. (2018), who argue that changes in RH in the southern-hemisphere extra-tropics are a large source of model spread; here we emphasize how and why such effects are also substantial in the tropics.

The idea that the climate response is sensitive to the particular distribution of relative humidity being held fixed, can be thought of as a form of state dependence. Most studies addressing this issue adopt a conceptual framework that only admit surface temperature as a state variable (Meraner et al., 2013; Knutti et al., 2017). RH plays no role. The limitation of such an assumption becomes obvious once one considers the climate sensitivity of an atmosphere with RH = 0. Hence, neglecting humidity as a state variable either implies that RH is known and constant, in which case the temperature might only be a proximate cause of the change in climate sensitivity, or that the limit of a dry atmosphere is singular.

In the present article we report on our investigation of the influence of RH on climate sensitivity using a 1D radiative-convective equilibrium (RCE) model, and highlight a phenomenon we call humidity–dependence. Such a model is attractive for our purposes because it captures (often with surprising fidelity) the behavior of more elaborated descriptions of the climate system in a physically transparent manner. In §2 we describe the model and methods. In §3 we compute the relative impact of a perturbation in the profile at different levels, as a function of RH. In §4 we simulate less idealized profiles of RH to understand and better quantify their effect on on the spread in clear-sky climate sensitivity produced by more elaborated models. In §5 we return to the trends in the reanalysis RH to quantify their implications for our understanding of the clear-sky climate sensitivity. We conclude in §6.

2 Model & Methods

Calculations were performed using the 1D-RCE model konrad (Kluft et al., 2019; Dacie et al., 2019). We adopt a configuration that uses the RRTMG radiative scheme (Mlawer et al., 1997) and a hard convective adjustment (Dacie, 2020) following the moist adiabatic lapse rate. Only clear-sky calculations are performed. In a subset of calculations discussed at the beginning of §3, we also used a uniform lapse rate. We used 500 pressure levels between 1000 hPa and 0.5 hPa. Following the prescription of the Radiative Convective Equilibrium Model Intercomparison Project, RCEMIP (Wing et al., 2018), the solar constant is set to $551.58\,\mathrm{W\,m^{-2}}$ and the zenith angle to $42.05°$, resulting in an insolation of $409.6\,\mathrm{W\,m^{-2}}$. The surface albedo is 0.2, and the ozone profile is coupled to the cold-point tropopause. The RH follows a prescribed vertical distribution up to the cold-point above which the specific humidity is kept uniform at its cold-point value. The RH is defined with respect to saturation over water above 0 °C and with respect to saturation over ice below −23 °C. In between, a combination of both are used (ECMWF, 2018).

A *run* is defined by its RH profile. It is composed of two equilibrium computations: (i) a spin-up with a constant surface temperature $T_0 = 300\,\mathrm{K}$, (ii) a new equilibrium after applying a sudden doubling of the CO_2 concentration. In (ii) the surface has no longer a fixed temperature but a fixed enthalpy sink, whose value is the top of the atmosphere radiative imbalance at the end of the spin-up, as Kluft (2020) argues to be best practice. The Equilibrium Climate Sensitivity, $\mathcal{S}$ of our model is defined as the difference between the second equilibrium surface temperature and T_0.

In §3, we discuss *perturbation runs*. In these, the tropospheric RH profile is uniform except for a 600 m thick layer, where the RH is increased or decreased (the perturbation). A perturbation run is thus defined by a base RH, a perturbation pressure, and a perturbation intensity δ_{RH}. The corresponding 'run' without perturbation is called a *control run*. This is illustrated in Fig. 2.

As a measure of the impact of a perturbation, we define the amplification factor a as the ratio of the $\mathcal{S}$ in the perturbation run, $\mathcal{S}_\mathrm{p}$, to the $\mathcal{S}$ in the corresponding control run, $\mathcal{S}_\mathrm{c}$:

$$a = \frac{\mathcal{S}_\mathrm{p}}{\mathcal{S}_\mathrm{c}} - 1. \tag{1}$$

In reanalysis data, see Fig. 1, the RH profiles peak in the boundary layer and in the upper-troposphere and show a distinct minimum in the mid-troposphere. For this reason, we call such a profile *C-shaped*. In order to simulate a C-shaped RH profile, we developed the following piecewise model, in pressure coordinates (shown in Fig. 4):

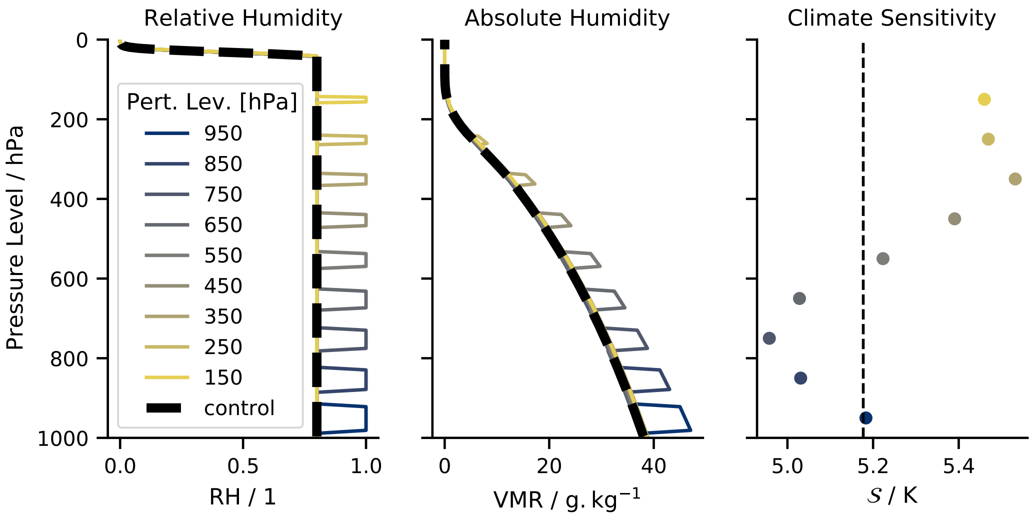

Figure 2. Illustration of the *perturbation runs* method. The control run, with a base RH of 0.8, is shown in dashed black. Each color corresponds to a run with a perturbation $\delta_{RH} = 0.2$ at a different level. The two left panels show the relative and absolute humidity profiles. The right panel shows $\mathcal{S}$ for each *perturbation run* as a function of perturbation pressure alongside the value of $\mathcal{S}$ for the control run (dashed vertical line).

- Linear in the boundary layer, from the surface to the lower-tropospheric peak (low point);
- Quadratic in the mid-troposphere, defined by 3 points: the two peaks and the humidity at 500 hPa (mid point);
- Linear above the upper-tropospheric peak, defined by the upper-tropospheric peak (top point) and the cold-point.

The advantages of such an RH profile is that it is defined by only 5 points, corresponding to parameters that are straightforward to interpret, and it catches the main feature of a realistic profile better than a uniform profile. Moreover, these parameters give us enough degrees of liberty to fit well AMIP and RCEMIP data, as detailed in §4.

3 Humidity–Dependence of $\mathcal{S}$

As a first set of experiments, we perform runs with different uniform tropospheric RH profiles, and for uniform and moist adiabatic lapse rates. Values of $\mathcal{S}$ for these runs are plotted in Fig. 3 (top panel). We find a robust increase in $\mathcal{S}$ with a moister troposphere. We decomposed $\mathcal{S}$ into contributions from the forcing and the feedback following Gregory et al. (2004). This shows that changes in $\mathcal{S}$ arise from changes in feedback as the forcing tends to be much smaller and of the opposite sign.

Let us use the effective emission height concept for the interpretation of our calculations. Let Φ_e be Earth's infrared irradiance at the top of the atmosphere. It can be associated with radiant power emitted by a black body at a temperature, T_e, such that $\Phi_\mathrm{e} = \sigma T_\mathrm{e}^4$, where σ is the Stefan-Boltzmann constant. We define the *effective emission height* to be the altitude z_e such that $T(z_\mathrm{e}) = T_\mathrm{e}$. These ideas can be generalized to allow for spectrally specific effective emission heights (Seeley & Jeevanjee, 2021), i.e., $z_{\mathrm{e},\lambda}$ with λ denoting some wavelength or spectral interval.

To help understand the water vapor feedback, we first apply this concept to a case with a uniform lapse rate, $\mathrm{d}T/\mathrm{d}z = -\Gamma$, and grey radiation characterized by a single emission height. If an initial (positive) perturbation in CO_2 causes an increase in the emission height $\delta z_{\mathsf{e,i}} > 0$, it would lead to a decrease in the emission temperature, $\delta T_{\mathsf{e,i}} = -\Gamma \delta z_{\mathsf{e,i}}$. This leads to a deficit in the Φ_{e}, and hence a positive radiative forcing. To balance the reduced emission, the troposphere (and surface) warms until the temperature at $z_{\mathrm{e}}+\delta z_{\mathrm{e}}$ adjusts to the value it previously had at z_{e}. As a reaction to this warming, if RH is to remain fixed, the absolute humidity must increases following the Clausius-Clapeyron law. The increase in e will in turn lead to a further change in z_{e}, which must be balanced by further warming, increasing humidity, and so on. $\mathcal{S}$, is the sum of the response from the initial forcing, plus this water vapor feedback.

Clausius-Clapeyron implies that

$$\delta e = RH \frac{\ell_{\mathrm{v}} e_{\mathrm{s}}}{R_{\mathrm{v}} T^2} \delta T, \tag{2}$$

where ℓ_{v} is the vaporization enthalpy, an R_{v} the water vapor gas constant. Eq. (2) shows that $\delta e \propto \mathrm{RH}$, which explains the linear relation between the $\mathcal{S}$ and the tropospheric RH for a given initial forcing ($2\times CO_2$), e.g., as displayed by the blue points in Fig. 3.

A non-uniform lapse rate – as is the case for the moist adiabat, whereby Γ is a monotonically increasing function of T – gives rise to additional effects. One is the well known lapse rate feedback. Another is a moister atmosphere: a troposphere whose surface and cold point temperatures are spanned by a moist adiabatic, rather than a uniform, lapse rate, will be warmer everywhere, and hence moister for the same RH. A further effect is that the vertical distribution of absolute humidity will be more bottom heavy, falling off less with height in the lower troposphere, where the moist adiabat is less than its mean value, and more with height, where the moist adiabat is greater than its mean value. The ability of an atmosphere with a moist adiabatic temperature profile to sample higher absolute humidities results in a strong increase in the water vapor feedback at high RH. This effect is particularly strong in our example because at the given value of T_0 the atmospheric window looses its transparency (Koll & Cronin, 2018) at high humidities, a self-amplifying affect that explains the sharp increase in $\mathcal{S}$ as RH increases for the moist adiabatic versus the uniform lapse rate runs (Fig. 3). Repeating our calculations with a smaller T_0 reduces the sensitivity to RH (not shown). For most values of RH, however, the moist adiabatic runs have a smaller $\mathcal{S}$, even more so if one uses the integrated water vapor (IWV) as the control variable, as shown by the points highlighted in on Fig. 3. This is mostly indicative of the importance of the lapse rate feedback. Calculations (not shown) that use a 'fixed' moist adiabatic lapse rate, i.e., one not allowed to change with surface warming, also have a slightly reduced $\mathcal{S}$ as compared to calculations adopting a uniform lapse rate with the same value of IWV. This suggests that the shape of the humidity profile also influences $\mathcal{S}$.

To assess how the shape of the RH profile influences $\mathcal{S}$ we perform perturbation runsm as described in §2 (see also Fig. 2). Perturbation runs are performed with $\delta_{\mathsf{RH}} = -0.1, 0.1, 0.2$. From these the amplification factor, a per Eq. 1, is related to δ_{RH} through linear regression. Fig. 3 plots a from its regressed slope multiplied by $\delta_{\mathsf{RH}} = 0.1$. Values are calculated for RH perturbations applied every 50 hPa to an otherwise constant RH profile. This sequence of height varying perturbation runs is computed for $0.4 \leq \mathrm{RH} \leq 0.8$ The impact of a positive RH perturbation is small, but discernibly positive (increasing $\mathcal{S}$) in the upper troposphere, and negative (decreasing $\mathcal{S}$) in the lower troposphere. The higher the base RH, the stronger is the sensitivity to the humidity perturbation. Moreover, the level of sign change rises with base RH.

The perturbation runs are consistent with our earlier discussion, but not especially intuitive. To understand them, and test their robustness, we performed line-by-line radiative transfer using the ARTS model (not shown) (Buehler et al., 2018). We find two

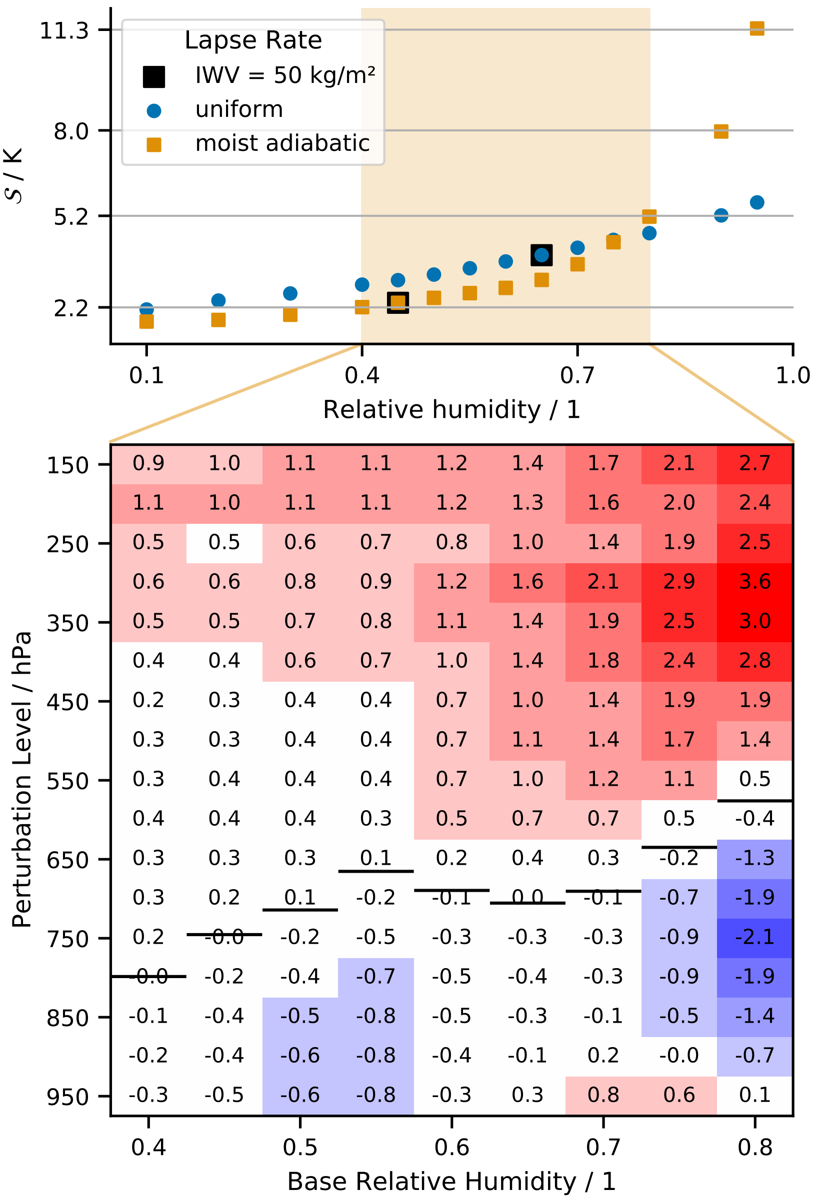

Figure 3. (Upper panel) $\mathcal{S}$ for different uniform tropospheric RH, and for experiments with a uniform tropospheric lapse rate of $6.5\,\mathrm{K\,km^{-1}}$ or with a moist adiabatic lapse rate. Black squared points correspond to experiments were integrated water vapor (IWV) was the closest to $50\,\mathrm{kg\,m^{-2}}$. (Lower panel) Amplification factor a (in percent) for 0.1 RH perturbation for different humidities and different perturbation levels. Blue and red colors for changes larger than 0.5 % in magnitude are indicative of the value's range. Black lines represent the mid-tropospheric level at which a changes sign.

opposing effects. In spectral regions where $z_{\mathrm{e},\lambda}$ is near the height of the RH perturbation, the change in $z_{\mathrm{e},\lambda}$ as water-vapor adjusts to warming is lessened. It is as if the fixed perturbation height helps anchor $z_{\mathrm{e},\lambda}$. In spectral regions where the effective emission height is well below the RH perturbation, the change in $z_{\mathrm{e},\lambda}$ as water-vapor adjusts to warming is heightened – increasing the strength of the water vapor feedback. The first (damping) effect explains the reduction in $\mathcal{S}$ associated with RH perturbations in the lower troposphere. It is also apparent at strongly absorbing wave numbers (rotational and ro-vibrational bands) for the perturbations in the upper troposphere. But for the latter case this reduction in the water-vapor feedback by the perturbation is more than offset by the second (amplifying) effect whereby the perturbation in the upper atmosphere increases the changes in $z_{\mathrm{e},\lambda}$ in parts of the window-region ($400\,\mathrm{cm}^{-1} < \lambda < 1200\,\mathrm{cm}^{-1}$) where CO_2 does not dominate.

4 Implications for Model-Based Estimates of ECS

Given the non-linearity of these effects, generalization is not automatic. Here we check whether results of the previous section can also be identified for less idealized perturbations to RH profiles more similar to those observed and simulated by climate models. For this purpose we use C-shaped RH profiles as defined in §2. To reduce their degrees of liberty we additionally fix the low point to 925 hPa and set the slopes below the low point, and above the high point, to $2.0 \times 10^{-5}\,\mathrm{Pa}^{-1}$ and $-5.8 \times 10^{-5}\,\mathrm{Pa}^{-1}$ respectively. These values are the mean of the parameters when fitting to RCEMIP profiles (see following paragraphs). We additionally set the RH at the cold-point to be half its peak (upper-troposphere) value, the level of this cold-point being computed by konrad. Calculations (runs) were then performed to quantify the impact of changing the remaining parameters: Starting from a 0.7/0.4/0.85 (top/mid/low) profile, we: (i) shifted the whole profile; (ii) changed only the RH at the top of the atmosphere; (iii) changed only the humidity at 500 hPa; (iv) changed only the humidity in the lower atmosphere. Humidity profiles and resulting changes in $\mathcal{S}$ are presented in Fig. 4. Qualitatively the response to these perturbations agrees well with what was learned from the response to more idealized perturbations: (i & ii) $\mathcal{S}$ increases with an increase in the upper tropospheric RH, also when this is part of a general moistening; (iv) $\mathcal{S}$ decreases if RH increases are confined to the lower troposphere; and (iii) increases in RH in the middle troposphere lead to little change in $\mathcal{S}$, until a critical RH is reached at which point $\mathcal{S}$ increases markedly.

In a second step, we performed runs with RH profiles set to fit RCEMIP simulations using storm-resolving and general circulation models (Except for UKMO-CASIM whose humidity profile led to a runaway) on large domains with an SST of 300 K (Wing et al., 2020) and CMIP5 AMIP ensembles. The fit is done by retrieving the pressure and humidity of the five points defining our C-shaped profile. In particular, the low and top points coincide with the local maxima and the cold-point pressure is retrieved from the temperature profile. The mid point remains fixed at 500 hPa and the surface is taken as the lowest point available. This enables us to assess the effect of the humidity profile alone, all other things being equal.

With RCEMIP RH profiles, we find a ±26% variation around the mean $\mathcal{S}$ value. The spread in feedback is $-1.25\,\mathrm{W\,m^{-2}\,K^{-1}}$ to $-3\,\mathrm{W\,m^{-2}\,K^{-1}}$, slightly smaller but comparable to what is found by Becker and Wing (2020). We thus explain the surprisingly large spread in clear-sky sensitivity in RCEMIP as being in large part a response to different RH profiles simulated by the models. Becker and Wing (2020) attribute this intermodel spread in RH to different degrees of convective self-aggregation, hence our work suggests that different degrees of convective self-aggregation can influence the climate sensitivity, even if the convective self-aggregation does not change with warming.

From CMIP5 AMIP output, we retrieved mean profiles over the tropical oceans (equatorward of 30°) averaged over the entire simulated period. As compared to RCEMIP RH

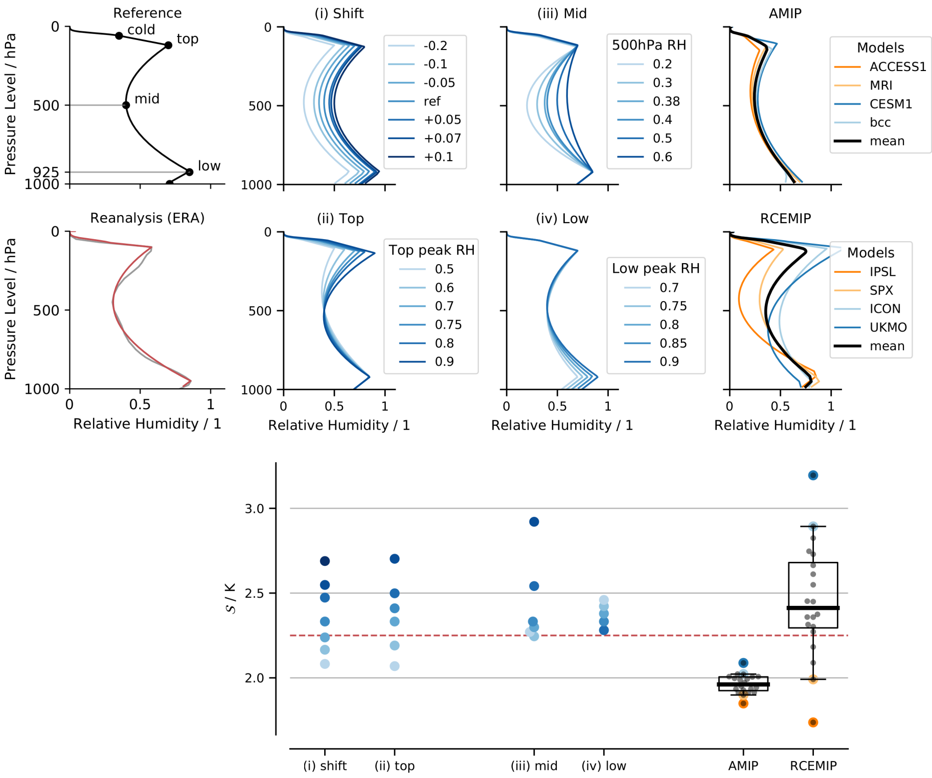

Figure 4. (Upper two rows) C-shaped RH profiles: Reference 0.7/0.4/0.85 (top/mid/low) profile (top-left); ERA5 profile as computed for §5 (grey), and corresponding C-shaped fit (red) (bottom-left). Four central panels correspond to the idealized experiments described in the first paragraph of §4. Two right-most panels display the mean and extreme profiles of the AMIP (top-right) and RCEMIP (bottom-right) datasets. (Lower panel) $\mathcal{S}$ for the idealized experiments and for the experiments with a profile fitted to the AMIP or RCEMIP ensembles. Boxplots' whiskers are set to display the 5th and 95th percentiles. On this graph and for statistics, only one point per model "family" (i.e. issued by the same institute) is used, corresponding to the average of all this family's models. Red dashed line correspond to the $\mathcal{S}$ computed with ERA5 C-shaped fit RH profile above.

profiles, those from the AMIP simulations are on average dryer, and thereby associated with a smaller $\mathcal{S}$. The drier AMIP profiles are indicative of large-scale circulations driven by differences in surface temperatures, i.e., Hadley and Walker cells which give rise to the dry tropics. The AMIP simulations differ less in their humidity profiles and likewise show less spread in $\mathcal{S}$, but even so differences approaching 10 % are evident

Given observations of the RH profiles in the atmosphere, it should be possible to correct model estimates of climate sensitivity using calculations such as ours. From a comparison of Fig. 1 and Fig. 4, we note that the RCE models tend to be moister than the observations, the AMIP simulations are drier. Fitting the C-shaped humidity profile to the observations yields an $\mathcal{S}$ of about 2.25 K; this is smaller than that of most RCE models, but larger than for the AMIP models. Likewise, ECS estimates in early calculations following the RH humidity profile used by Manabe and Wetherald (1967), would, due to an unrealistically dry upper atmosphere, be biased too low. However, for the lower humidities and temperatures used in that study, the fixed lapse assumption actually over compensates, leading to a larger sensitivity as seen in Kluft et al. (2019). This, along with the upper panel of Fig. 3, is illustrative of how the lapse rate feedback depends on the base state RH.

5 Impact of RH Trends in Reanalysis Data

Based on the above analysis we return to our initial question, which is how to interpret RH trends in the reanalysis products. The profiles presented in Fig. 1 are from the ERA5 (Hersbach et al., 2020), and the JRA-55 (Kobayashi et al., 2015) reanalyses of the past forty years (1979-2019) of meteorological observations. Relative and absolute humidity, as well as temparature, are averaged over tropical oceans (equatorward of 30°). Trends regressed from monthly data are significant at several levels and consistent across both reanalyses. They are also evident in the difference between the mean profile in the first and last decade (not shown). We were surprised that RH at low levels was robustly decreasing – something that merits further investigation – even if averaged over height $\delta RH \approx 0$. Our analysis does not tell us how strongly these trends influence the expected warming over the past forty years, but it does tell us that the pattern of change, with moistening aloft and drying in the lower middle troposphere is conditioning the climate system toward greater sensitivity.

6 Conclusions

The response of the atmosphere to radiative forcing as a function of the assumed profile of relative humidity (RH) is explored using a one-dimensional radiative-convective equilibrium model. For profiles chosen to sample the range produced by state of the art climate and storm-resolving models run under idealized conditions, the calculated equilibrium climate sensitivity of our model ($\mathcal{S}$) varies between 2 K to 3 K, depending on the RH profile, highlighting a humidity–dependence of the climate sensitivity: Moister atmospheres were shown to have a larger $\mathcal{S}$, increasingly so with warmer temperature, consistent with understanding of how water vapor influences the transmissivity of the atmospheric window (Nakajima et al., 1992; Koll & Cronin, 2018; Seeley & Jeevanjee, 2021). $\mathcal{S}$ is further shown to increase with increasing humidity in the upper troposphere, but decreases with increases in humidity in the lower mid-troposphere.

The use of a simple physical model, konrad, makes it easier to understand the basic physics determining the outcome of our calculations. For instance, with the chosen framework it is possible to show how the the lapse rate's influence on the total amount and vertical distribution of humidity for a given profile of RH influences $\mathcal{S}$. We could also investigate how $\mathcal{S}$ depends on the shape of the RH profile, which expresses competing effects, whereby perturbations to the humidity can both reduce or increase the change in the emission height associated with changes in absolute humidity to maintain a constant relative humidity with warming. The former effect dominates when the humidity perturbation is near the emission height resulting in a slight reduction in $\mathcal{S}$ for bottom heavy humidity profiles.

Our work emphasizes the importance of realistically representing the relative humidity profile when calculating climate sensitivity. Models that are too humid, particularly in the mid- and upper-troposphere will have larger sensitivities, an effect which will amplify with increased warming. Convective self-aggregation modifies the mean relative humidity profile, thereby reducing ECS, even if the degree of convective aggregation itself does not change with warming. In this context, our study also encourages the use of RH as metric for the fidelity of the moist physics in climate models. To the extent climate models are unable to realistically represent the observed distribution of RH, our methods may make it possible to estimate the quantitative effect of these biases.

Humidity profiles over tropical oceans as represented in reanalysis products, tend to be moister than those produced by models forced with observed SSTs, implying a larger clear-sky sensitivity. Three dimensional radiative convective equilibrium models, which are more physical – but less constrained by large-scale sea-surface temperature gradients – tend to be more humid, but also have more divergent humidity profiles.

Surprisingly large changes in RH are reported by the reanalysis products over the last forty years, changes which our calculations suggest will condition the climate system to be more sensitive to forcing in the future. This finding adds an additional dimension to Knutti and Rugenstein's (2015) statement that the feedback parameter is not constant, and that non-linearity in the system may be important when assessing Earth's equilibrium climate sensitivity. The surprising trends in the reanalysis humidity products, particularly the drying in the tropical lower troposphere, reminds us of Held and Soden's plea to be attentive to this issue, and merits the renewed attention of experts.

Acknowledgments

Authors acknowledge the financial surpport of the Max-Planck Gesellschaft. S.B. also benefited from the French state aid managed by the ANR under the "Investissements d'avenir" programme with the reference ANR-11-IDEX-0004 - 17-EURE-0006. B.S. and L.K. acknowledge support from the European Union's Horizon 2020 Research and Innovation Programme under grant agreement No. 820829 (CONSTRAIN Project). We thank Tobias Becker, Sally Dacie, Didier Paillard, Maria Rugenstein and Catherine Stauffer for helpful scholar discussion concerning this study, and Hauke Schmidt's GCC group at MPI-M for advice and feedback. We are also grateful to Sébastien Fromang and Theresa Lang for their review of the present manuscript.

- Primary data including simulation scripts and code for reproducing the figures are available on Zenodo through `https://doi.org/10.5281/zenodo.4423268`.
- konradv0.8.1 is available at `github.com/atmtools/konrad`, and latest sources are available at `https://doi.org/10.5281/zenodo.4434837`.
- ERA5 data is available on the Copernicus Climate Change Service Climate Data Store (CDS, `https://cds.climate.copernicus.eu/cdsapp#!/dataset/reanalysis-era5-pressure-levels-monthly-means?tab=overview`).
- JRA-55 data were retrieve from `https://jra.kishou.go.jp/JRA-55/index_en.html`.
- The German Climate Computing Center (DKRZ) hosts the standardized RCEMIP and CMIP5-AMIP output (`https://cera-www.dkrz.de/WDCC/ui/cerasearch/info?site=RCEMIP_DS`).

The authors declare no conflict of interest.

References

Becker, T., & Wing, A. A. (2020). Understanding the extreme spread in climate sensitivity within the radiative-convective equilibrium model intercomparison project. *Journal of Advances in Modeling Earth Systems*, *12*(10). doi: 10.1029/2020MS002165

Buehler, S. A., Mendrok, J., Eriksson, P., Perrin, A., Larsson, R., & Lemke, O. (2018). ARTS, the atmospheric radiative transfer simulator — version 2.2, the planetary toolbox edition. *Geoscientific Model Development*, *11*(4), 1537–1556. doi: 10.5194/gmd-11-1537-2018

Charney, J. G., Arakawa, A., Baker, D. J., Bolin, B., Dickinson, R. E., Goody, R. M., … Wunsch, C. I. (1979). *Carbon dioxide and climate: a scientific assessment*. National Academy of Sciences, Washington, DC.

Dacie, S. (2020). *Using simple models to understand changes in the tropical mean atmosphere under warming* (Unpublished doctoral dissertation). University of Hamburg, Hamburg.

Dacie, S., Kluft, L., Schmidt, H., Stevens, B., Buehler, S. A., Nowack, P. J., ... Birner, T. (2019). A 1D RCE Study of Factors Affecting the Tropical Tropopause Layer and Surface Climate. *Journal of Climate*, *32*(20), 6769–6782. doi: 10.1175/JCLI-D-18-0778.1

ECMWF. (2018). Part iv : Physical processes. In *Ifs documentation cy45r1.* Author. Retrieved from `https://www.ecmwf.int/node/18714`

Gregory, J. M., Ingram, W. J., Palmer, M. A., Jones, G. S., Stott, P. A., Thorpe, R. B., ... Williams, K. D. (2004). A new method for diagnosing radiative forcing and climate sensitivity. *Geophysical Research Letters*, *31*(3). doi: 10.1029/2003GL018747

Held, I. M., & Soden, B. J. (2000). Water Vapor Feedback and Global Warming. *Annual Review of Energy and the Environment*, *25*(1). doi: 10.1146/annurev.energy.25.1.441

Hersbach, H., Bell, B., Berrisford, P., Hirahara, S., Horányi, A., Muñoz-Sabater, J., ... others (2020). The era5 global reanalysis. *Quarterly Journal of the Royal Meteorological Society*, *146*(730), 1999–2049.

Kluft, L. (2020). *Benchmark Calculations of the Climate Sensitivity of Radiative-Convective Equilibrium* (Doctoral dissertation, Universität Hamburg, Hamburg). doi: 10.17617/2.3274272

Kluft, L., Dacie, S., Buehler, S. A., Schmidt, H., & Stevens, B. (2019). Re-examining the first climate models: Climate sensitivity of a modern radiative-convective equilibrium model. *Journal of Climate*, *32*, 8111–8125. doi: 10.1175/JCLI-D-18-0774.1

Knutti, R., & Rugenstein, M. A. A. (2015). Feedbacks, climate sensitivity and the limits of linear models. *Philosophical Transactions of the Royal Society A: Mathematical, Physical and Engineering Sciences*, *373*(2054), 20150146. doi: 10.1098/rsta.2015.0146

Knutti, R., Rugenstein, M. A. A., & Hegerl, G. C. (2017). Beyond equilibrium climate sensitivity. *Nature Geoscience*, *10*(10), 727–736. doi: 10.1038/ngeo3017

Kobayashi, S., Ota, Y., Harada, Y., Ebita, A., Moriya, M., Onoda, H., ... others (2015). The jra-55 reanalysis: General specifications and basic characteristics. *Journal of the Meteorological Society of Japan. Ser. II*, *93*(1), 5–48.

Koll, D. D. B., & Cronin, T. W. (2018). Earth's outgoing longwave radiation linear due to H2O greenhouse effect. *Proceedings of the National Academy of Sciences*, *115*(41), 10293–10298. doi: 10.1073/pnas.1809868115

Manabe, S., & Wetherald, R. T. (1967). Thermal Equilibrium of the Atmosphere with a Given Distribution of Relative Humidity. *Journal of the Atmospheric Sciences*, *24*, 241–259. doi: 10.1175/1520-0469(1967)024⟨0241:TEOTAW⟩2.0.CO;2

Medeiros, B., Stevens, B., Held, I. M., Zhao, M., Williamson, D. L., Olson, J. G., & Bretherton, C. S. (2008). Aquaplanets, climate sensitivity, and low clouds. *Journal of Climate*, *21*(19), 4974 – 4991. doi: 10.1175/2008JCLI1995.1

Meraner, K., Mauritsen, T., & Voigt, A. (2013). Robust increase in equilibrium climate sensitivity under global warming. *Geophysical Research Letters*, *40*(22), 5944–5948. doi: 10.1002/2013GL058118

Mlawer, E. J., Taubman, S. J., Brown, P. D., Iacono, M. J., & Clough, S. A. (1997). Radiative transfer for inhomogeneous atmospheres: RRTM, a validated correlated-k model for the longwave. *Journal of Geophysical Research: Atmospheres*, *102*(D14), 16663–16682. doi: 10.1029/97JD00237

Nakajima, S., Hayashi, Y.-Y., & Abe, Y. (1992, December). A Study on the ?Runaway Greenhouse Effect? with a One-Dimensional Radiative?Convective Equilibrium Model. *Journal of Atmospheric Sciences*, *49*(23), 2256–2266. doi:

10.1175/1520-0469(1992)049⟨2256:ASOTGE⟩2.0.CO;2

Pierrehumbert, R. T. (1995, May). Thermostats, Radiator Fins, and the Local Runaway Greenhouse. *J. Atmos. Sci*, *52*(1), 1784–1806.

Po-Chedley, S., Armour, K. C., Bitz, C. M., Zelinka, M. D., Santer, B. D., & Fu, Q. (2018). Sources of Intermodel Spread in the Lapse Rate and Water Vapor Feedbacks. *Journal of Climate*, *31*(8), 3187–3206. doi: 10.1175/JCLI-D-17-0674.1

Seeley, J. T., & Jeevanjee, N. (2021). H_2O windows and CO_2 radiator fins: a clear-sky explanation for the peak in ecs. *Geophysical Research Letters*, *n/a*(n/a), e2020GL089609. Retrieved from `https://agupubs.onlinelibrary.wiley.com/doi/abs/10.1029/2020GL089609` (e2020GL089609 2020GL089609) doi: https://doi.org/10.1029/2020GL089609

Sherwood, S., Webb, M. J., Annan, J. D., Armour, K. C., Forster, P. M., Hargreaves, J. C., … Zelinka, M. D. (2020). An assessment of Earth's climate sensitivity using multiple lines of evidence. *Reviews of Geophysics*. doi: 10.1029/2019RG000678

Soden, B. J., & Held, I. M. (2006). An assessment of climate feedbacks in coupled ocean-atmosphere models. *Journal of Climate*, *19*(14), 3354–3360. doi: 10.1175/JCLI3799.1

Stevens, B., Sherwood, S. C., Bony, S., & Webb, M. J. (2016). Prospects for narrowing bounds on Earth's equilibrium climate sensitivity. *Earth's Future*, *4*(11), 512–522. doi: 10.1002/2016EF000376

Vial, J., Dufresne, J.-L., & Bony, S. (2013). On the interpretation of inter-model spread in CMIP5 climate sensitivity estimates. *Climate Dynamics*, *41*(11), 3339–3362. doi: 10.1007/s00382-013-1725-9

Wing, A. A., Reed, K. A., Satoh, M., Stevens, B., Bony, S., & Ohno, T. (2018). Radiative-convective Equilibrium Model Intercomparison Project. *Geoscientific Model Development*, 793–813.

Wing, A. A., Stauffer, C. L., Becker, T., Reed, K. A., Ahn, M.-S., Arnold, N. P., … Zhao, M. (2020). Clouds and Convective Self-Aggregation in a Multimodel Ensemble of Radiative-Convective Equilibrium Simulations. *Journal of Advances in Modeling Earth Systems*, *12*(9), e2020MS002138. doi: https://doi.org/10.1029/2020MS002138